Proceedings of the ASME 2010 International Design Engineering Technical Conferences & Computers and Information in Engineering Conference
IDETC/CIE 2010
August 15-18, 2010, Montreal, Quebec, Canada

DETC2010-29190

MODELING THE COMPLIANCE OF A VARIABLE STIFFNESS C-SHAPED LEG USING CASTIGLIANO'S THEOREM

Yasemin Ö. Aydın*
Department of Electrical and
Electronics Engineering
Middle East Technical University
Ankara,TURKEY 06531
Email: yasemino@eee.metu.edu.tr

Kevin C. Galloway
Mechanical Engineering
and Applied Mechanics
University of Pennsylvania
Philadelphia, PA 19104
Email: kcg@seas.upenn.edu

Yigit Yazicioglu
Department of Mechanical Engineering
Middle East Technical University
Ankara,TURKEY 06531
Email: yigit@metu.edu.tr

Daniel E. Koditschek
Department of Electrical and System Engineering
University of Pennsylvania
Philadelphia, PA 19104
Email: kod@seas.upenn.edu

ABSTRACT

This paper discusses the application of Castigliano's Theorem to a half circular beam intended for use as a shaped, tunable, passively compliant robot leg. We present closed-form equations characterizing the deflection behavior of the beam (whose compliance properties vary along the leg) under appropriate loads. We compare the accuracy of this analytical representation to that of a Pseudo Rigid Body (PRB) approximation in predicting the data obtained by measuring the deflection of a physical half-circular beam under the application of known static loads. We briefly discuss the further application of the new model for solving the dynamic equations of a hexapod robot with a C-shaped leg.

1 INTRODUCTION

This paper describes our effort to characterize the compliant properites of constant and tunable stiffness C-shaped legs for RHex-like running robots. RHex is a bioinspired robot that utilizes six compliant legs to store and return energy, enabling fast and efficient running on a great variety of natural terrain [1,2] (see Edubot in Fig. 1, which is a smaller version of RHex). While the C-leg has proven very successful in the field [3], the very same complicated, spatial compliance properties that confer such great advantage in the running application present a special challenge for those who, like us, motivated by the hope of more rational robot design, seek a useful dynamical model of the locomotion it affords. Presently, suitable running gaits for a given leg stiffness and payload are identified empirically [4]. As one important step toward the development of a more analytically informed design methodology, we desire a simple, lumped parameter model that can 1) capture the elastic behavior of a C-leg more accurately (both constant stiffness and variable stiffness configurations) and 2) can be used to capture the dynamics of a running hexapod.

Modeling the deflections of a curved elastic element presents several challenges — the first and foremost being the selection of a suitable model. There are several ap-

*Address all correspondence to this author.

proaches one could employ including the *Finite Element* method (FE), the chain algorithm, and the *Pseudo-Rigid-Body* (PRB) model to name a few. The FE method is probably the most common due to its explicit incorporation into many 3D modeling programs. An elastic element is divided into a finite number of discrete sub-elements [5] whereby the behaviour of each element is expressed in terms of nodal forces and moments. This approach tends to be computationally expensive and requires a larger investment of time to optimize a flexure geometry for given loading conditions. The *Chain Algorithm* is another numerical method which discretizes an elastic element into smaller elements which are analyzed in succession [6]. This method is computationally less expensive than FE method though it presents some challenges in defining the boundary conditions. Both methods offer reliable, accurate numerical representation of complex geometries and loading conditions that would otherwise be impossible to analyze with any confidence using a closed form solution [6]. However, presented as we are in this problem with simple geometries that experience moderate amount of deflections that lend themselves to closed form models would be preferable because of the greater parametric insight they lend, if one could be confident in their accuracy.

One simple closed form approach is the *Pseudo-Rigid-Body* (PRB) model, which approximates the deflection behaviour of an elastic member as two rigid links that are connected by a torsional spring [6,7]. The torsional spring and the lengths of the rigid links are used to characterize the stiffness of the member and the deflection path of the loading point. This approach has been used in our previous studies [8, 9] to capture the spatial compliant properties of an initially curved beam.

In [9], we present a tunable stiffness C-leg using the method of structure-controlled stiffness whereby the stiffness of the C-leg is adjusted by moving a compliant slider along the length of the leg (see Fig. 2). In its simplest form this can be viewed as an intially curved, stepped cantilever beam. Capturing the spatial compliance of this structure with the PRB model presents a special challenge as this model assumes a thin elastic element of constant cross-section.

In this paper, we present an energy based deflection analysis method, based upon *Castigliano's Theorem* [10], that is capable of characterizing the spatial compliance of an initially curved, stepped cantilever beam. The theorem states that the deflection of any point on a beam is equal to the partial derivative of total strain energy of the beam with respect to external forces on that point. Castigliano's Theorem is useful when the strain energy of the structure can be easily expressed in terms of external forces. For the leg geometry we are considering, it is simple to implement

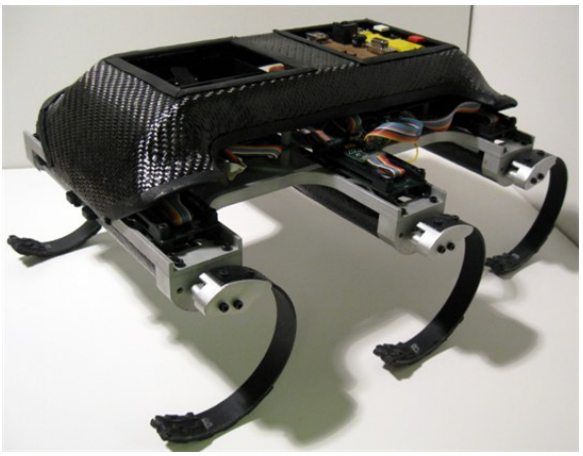

FIGURE 1. EDUBOT [11]

and computationally more efficient compared to numerical methods. Taking this point of view, we propose in this paper a new curved leg compliance model that characterizes the spatial compliance of the C-leg as a function of external forces.

The organization of the paper is as follows: in Section 2, we describe the implementation of Castigliano's Theorem for the force-deflection analysis of a variable stiffness C-leg. Section 3 presents the experimental setup used in this study and Section 4 compares the performance of the Castigliano and PRB models with experimental data. In Section 5 we close with a summary of the work and a discussion of future work.

2 CASTIGLIANO'S THEOREM

In this section, we employ Castigliano's Theorem [10] to model the deflection path of an elastic curved beam under the effect of external forces. This theorem states that the displacement resulting from any force (or moment) is determined by obtaining the partial derivative of the total strain energy with respect to that force [12, 13]. The first step, therefore, is to calculate the resulting strain energy for a given load which is expressed as

$$U = \int \frac{M^2 R\, d\gamma}{2AeE} + \int \frac{F_\theta^2 R\, d\gamma}{2EA} + \int \frac{C F_R^2 R\, d\gamma}{2AG} - \int \frac{M F_\theta\, d\gamma}{AE} \quad (1)$$

where M, F_θ, and F_R are the total bending moment, tangential and radial forces, respectively, that are created by the applied forces at the cross section of the curved beam. It should be noted that

TABLE 1. TABLE OF VARIABLES USED IN EQN. 1

Variable	Definition	Unit
A	cross-section area	m^2
E	young's modulus	GPa
e	eccentricity	m
G	shear modulus	GPa
R	radius of curvature	m
I	second moment of area	m^4
C	correction factor	unitless

$$dl = R\, d\gamma \tag{2}$$

where R is the radius and l is the arc length of the curved element. The parameters in Eqn. (1) are listed in Tab. 1. The integration interval changes from the loading point to the fixed end of the curved beam. In general, the strain energy expression, Eqn. (1), can be approximated by Eqn. (3) if the radius of the curved beam is on the order of ten times larger than its thickness [12].

$$U \approx \int \frac{M^2 R\, d\gamma}{2EI} \tag{3}$$

The partial derivative of total strain energy, U in Eqn. (3), with respect to an arbitrary force F_i gives the deflection of the loading point, δ_i in the direction of the F_i,

$$\delta_i = \frac{\partial U}{\partial F_i} \tag{4}$$

2.1 Modeling a Tunable Stiffness C-leg

We now apply Castigliano's Theorem to the tunable stiffness C-leg shown in Fig. 2. In the proposed mechanical design presented in [9], the stiffness of the C-leg is adjusted by sliding a compliant curved member, known as the compliant slider, along the outside of the C-leg. This implementation of structure-controlled stiffness allows the sheathed and unsheathed portions of the C-leg to store and return strain energy. To calculate the strain energy stored in compliant leg, the forces and moments at the cross-section were algebraically expressed in terms of external forces F_x and F_y as shown in Fig. (3). Note that,

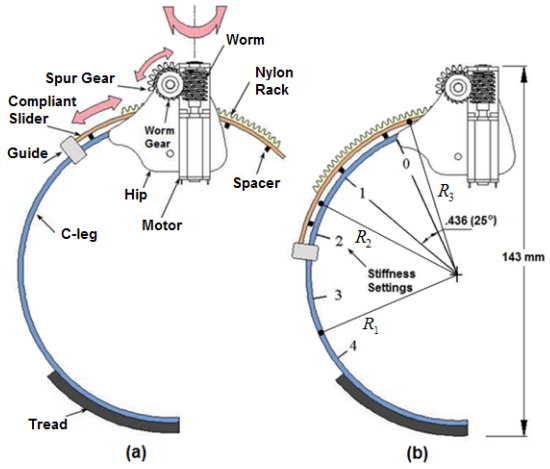

FIGURE 2. SIDE VIEW OF THE TUNABLE STIFFNESS C-LEG (PRESENTED WITH PERMISSION FROM [9])

the external force F_y is along the radius of the leg and F_x is perpendicular to F_y. The total bending moment, radial force and tangential force at the cross-section can be written as

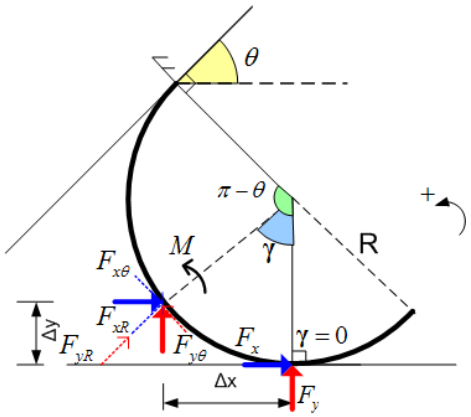

FIGURE 3. FORCES AND MOMENT AT CROSS-SECTION

$$M = F_x \Delta y + F_y \Delta x = F_x R(1 - cos(\gamma)) + F_y R sin(\gamma) \tag{5a}$$
$$F_R = F_{xR} + F_{yR} = F_x sin(\gamma) + F_y cos(\gamma) \tag{5b}$$
$$F_\theta = F_{x\theta} - F_{y\theta} = F_x cos(\gamma) - F_y sin(\gamma) \tag{5c}$$

As seen from Eqn. (5a-5c), the contact forces, F_x and F_y, determine the cross-sectional forces, F_θ and F_R, throughout the beam. Since in our case $\frac{R}{h_{leg}} > 10$ we used

the simpler form of strain energy expression, Eqn. (3), to express the strain energy stored in the tunable stiffness leg

$$U = \int_0^{\alpha_1} \frac{M^2 R_1 \, d\gamma}{2(EI)_{leg}} + \int_{\alpha_1}^{\alpha_2} \frac{M^2 R_2 \, d\gamma}{2(EI)_{eff}} + \int_{\alpha_2}^{\alpha_3} \frac{M^2 R_3 \, d\gamma}{2(EI)_{slider}} \quad (6)$$

TABLE 2. TABLE OF VARIABLES USED IN EQN. (6)

Variable	Definition	Equation
M	bending moment	Eqn. (5a)
R_1, R_2, R_3	radius of curvature	Eqn. (7)
$\alpha_1, \alpha_2, \alpha_3$	integral intervals	Eqn. (8)
$I_{leg}, I_{eff}, I_{slider}$	second moment of area of crosssection	Eqn. (10)
$E_{leg}, E_{eff}, E_{slider}$	young modulus	Tab. (3)

where Tab. 2 lists all the symbols and their defining equations. In our case R_1, R_2 and R_3 (depicted in Fig. 2) are almost equal to each other, and for simplicity, can be represented as a single radius value, R that is found by solving an explicit formula of a circle that passes through three points on the leg, which in this particular case is shifted Marker 1, Marker 2 and Marker 3 shown in Fig. 4,

$$R_1 = R_2 = R_3 = R \quad (7)$$

In this study we also assume that the circular leg geometry does not change after deflection. As depicted in Fig. 2, the compliant slider can move continuously along the leg's arc length from leg stiffness setting (LSS) = 0 to 4. This has the effect of dividing the leg into three arc lengths which are defined in Fig. 4 as $l(AB) = l_{free}$, $l(BC) = l_{slider}$, $l(CD) = l_{end}$. The integral intervals at any loading point can be written as

$$\alpha_1 = \frac{l_{free}}{R}, \quad \alpha_2 = \frac{(l_{free} + l_{slider})}{R}, \quad \alpha_3 = \frac{(l_{free} + l_{slider} + l_{end})}{R} = \pi - \theta \quad (8)$$

Note that θ is the angle of leg, which determines the point of contact of the leg with the ground, with respect to hip(see Fig. 3) and l_{slider} is the length of the compliant slider that equals to

TABLE 3. PROPERTIES OF LEG AND SLIDER

Variable	Definition	Value
b_{leg}, b_{slider}	width of the cross-section	18 mm
h_{leg}, h_{slider}	height of the cross-section	2.5 mm
R	radius of leg	57 mm
$E_{leg}, E_{slider}, E_{eff}$	young's modulus	9.65 GPa

$$l_{slider} = LSS \cdot l_s; \quad LSS \in \{0, 1, 2, 3, 4\} \quad (9)$$

where l_s is the arc length of slider at LSS=1. From points B to C in Fig. 4 the slider and leg deform together as separate but concentric beams (i.e. they are not rigidly connected to each other and are allowed to slide past one another) to increase the overall stiffness of the beam. The second moment of area of the leg covered by the compliant slider is calculated as [14]

$$I_{eff} = I_{leg} + I_{slider} \quad \text{where} \quad (10a)$$

$$I_{leg} = \frac{b_{leg} h_{leg}^3}{l2}, \quad I_{slider} = \frac{b_{slider} h_{slider}^3}{l2} \quad (10b)$$

The material and geometric properties of the leg and compliant slider are presented in Tab. 3.

The partial derivative of Eqn. (6) with respect to F_x and F_y gives us the deflection amount, $\delta = [\delta_x, \delta_y]$, of the loading point in the direction of the forces.

$$\delta_x = \frac{\partial U}{\partial F_x}, \quad \delta_y = \frac{\partial U}{\partial F_y} \quad (11)$$

Eqn. (11) can be represented in matrix form as

$$\begin{bmatrix} \delta_x \\ \delta_y \end{bmatrix} = \begin{bmatrix} c_{xx} & c_{xy} \\ c_{yx} & c_{yy} \end{bmatrix} \begin{bmatrix} F_x \\ F_y \end{bmatrix} = [C][F] \quad (12)$$

where the elements of compliance matrix, C, are,

$$
\begin{aligned}
c_{xx} &= \frac{R^3}{8}\Big(\frac{1}{(EI)_{leg}}(12\alpha_1 - 16sin(\alpha_1) + 2sin(2\alpha_1)) \\
&+ \frac{1}{(EI)_{eff}}(-12(\alpha_1-\alpha_2) + 16(sin(\alpha_1) - sin(\alpha_2)) \\
&- 2(sin(2\alpha_1) - sin(2\alpha_2))) + \frac{1}{(EI)_{slider}}(-12(\alpha_2-\alpha_3) \\
&+ 16(sin(\alpha_2) - sin(\alpha_3)) - 2(sin(2\alpha_2) - sin(2\alpha_3)))) \\
c_{xy} = c_{yx} &= \frac{R^3}{8}\Big(\frac{1}{(EI)_{leg}}(6 + 2(-4cos(\alpha_1) + cos(2\alpha_1))) \\
&+ \frac{1}{(EI)_{eff}}(8(cos(\alpha_1) - cos(\alpha_2)) - 2(cos(2\alpha_1) - cos(2\alpha_2))) \\
&+ \frac{1}{(EI)_{slider}}(8(cos(\alpha_2) - cos(\alpha_3)) - 2(cos(2\alpha_2) - cos(2\alpha_3)))) \\
c_{yy} &= \frac{R^3}{8}\Big(\frac{1}{(EI)_{leg}}(4\alpha_1 - 2sin(2\alpha_1)) \\
&+ \frac{1}{(EI)_{eff}}(-4(\alpha_1-\alpha_2) + 2(sin(2\alpha_1) - sin(2\alpha_2))) \\
&+ \frac{1}{(EI)_{slider}}(-4(\alpha_2-\alpha_3) + 2(sin(2\alpha_2) - sin(2\alpha_3)))) \qquad (13)
\end{aligned}
$$

Equation (12) expresses the deflection of the loading point as a linear function of external forces. The elements of the compliance matrix, C in Eqn. (12), are updated when the point of application of the load (i.e. leg angle θ) changes, as in the legged locomotion of the RHex robot, or the leg stiffness is manupulated by shifting the position of the compliant slider. Since α_1, α_2 and α_3 in Eqn. (13) depend on instantaneous leg angle, the elements of the compliance matrix are not constant during the motion and the leg acts as a variable stiffness spring. This new leg model can be substituted into the dynamic equations for a multi-legged robot with a C-shaped leg [2]. Furthermore, the stiffness matrix, which is the inverse of the compliance matrix, C, can be utilized to find the unknown external forces (such as ground reaction forces, friction forces and so forth) applied to the leg.

3 EXPERIMENTAL SETUP

In this study we empirically validate the deflection results predicted by Castigliano's Theorem by statically loading a tunable C-leg for a range of leg stiffness settings. Additionally, we present these results with those predicted by the PRB model as an added basis for comparison. In the experimental setup shown in Fig. 5, the hip portion of the fiberglass tunable stiffness C-leg was anchored to the platform of a linear stage, and the C-leg was allowed to cantilever from the platform. A Micos linear stage[1] and an AMTI HE6x6 multi-axis force plate were rigidly mounted to an aluminum base plate. A flexible, fixed length steel cable connected the force plate to an aluminum clamp that was fixed to the leg at Marker 2. A pulley was mounted to the hip to keep the cable normal to the force plate's surface. The force plate is capable of measuring up to 10 pounds with a 12-bit resolution[2]. The linear stage was commanded to travel 20 mm at 10mm/s. The deflection path of the leg was recorded using an Optotrak 3020 by tracking three IR markers that were mounted to the leg (see Fig. 5). The sampling rate of both the force plate and motion capture system was 200 Hz. Leg deflection and force data were collected for the discrete leg stiffness settings, LSS = 0 – 4, shown in Fig. 5.

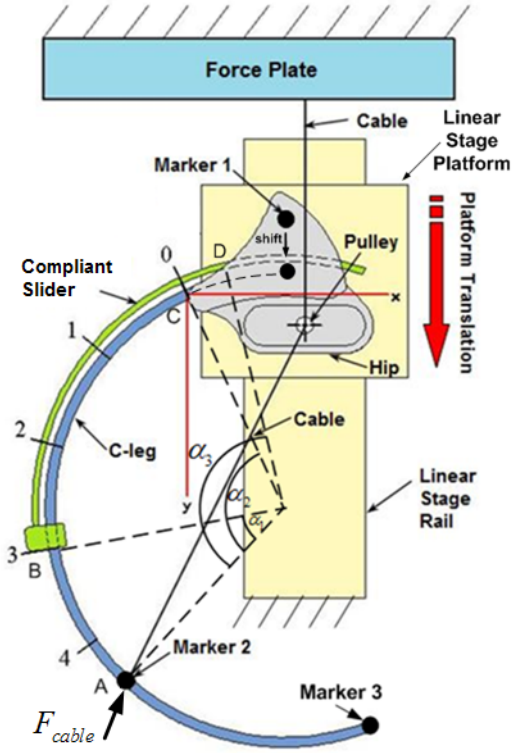

FIGURE 4. TOP VIEW OF THE EXPERIMENTAL SETUP IN WHICH THE HIP PORTION OF THE LEG IS RIGIDLY ATTACHED TO A LINEAR STAGE PLATFORM AND THE LEG IS DEFLECTED BY MOVING THE STAGE WHILE A FIXED LENGTH CABLE CONNECTS THE LEG TO A FORCE PLATE ANCHORED TO THE GROUND PLANE.

[1] See http://www.micos-online.com

[2] Additional information can be found at http://www.amti.biz

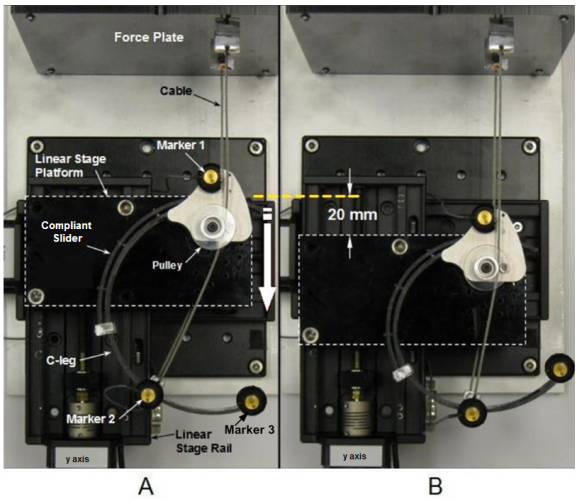

FIGURE 5. TOP VIEW OF EXPERIMENTAL SETUP. (a) INITIAL POSITION OF UNDEFLECTED LEG (b) DEFLECTED LEG (PRESENTED WITH PERMISSION FROM [9])

4 FORCE-DEFLECTION RESULTS

In Fig. 6, we present the actual and estimated deflection path of loading point A (see Fig. 4) and percentage errors (Fig. 6-c,d) of the two models. Since the current PRB model is not capable of estimating deflection behaviour of the leg for intermediate stiffness settings, we only compared the results of two extreme stiffness (LSS = 0 and 4). The *percentage error* of two models is defined as follows:

$$PE(i) = \frac{\sqrt{(x(i)_{act} - x(i)_{est})^2 + (y(i)_{act} - y(i)_{est})^2)}}{d_{max}}.100\%, \quad (14)$$

from $i = 1 : n$, where x-y is the position of loading point in the coordinate frame that is attached to point C in Fig. 4, n is the number of samples and d_{max} is the magnitude of actual maximum deflection. The results show that, at the LSS = 0 (Fig. 6-a), Castigliano's method gives smoother error over the whole deflection range while the error of PRB model increases gradually. At maximum deflection, the percentage error of PRB model is 2.5 times larger than the error of Castigliano's model. On the other hand two models produce almost same error at the stiffest setting, LSS4 (Fig. 6-b). This indicates that as the compliance of the leg decreases, the deflection behaviour of the leg is estimated with similar accuracy by both models.

Figure 7-a,b,c presents the actual and estimated deflection path of loading point for the intermediate stiffness settings. As seen from the figure, Castigliano's model is capable of accurate prediction of deflection path for various stiffness settings.

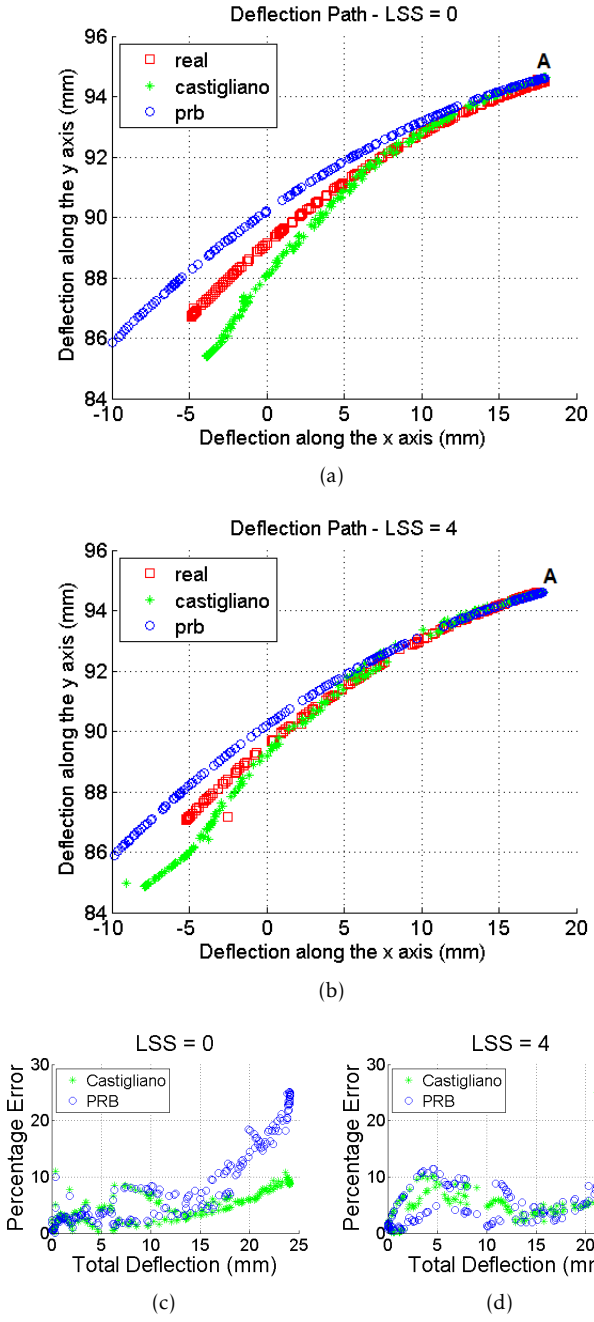

FIGURE 6. (a)-(b) COMPARISION OF THE DEFLECTION PATH OF PRB AND CASTIGLIANO MODEL WITH REAL DATA AT THE STIFFNESS EXTREMES, LSS0 AND LSS4. (c)-(d) PERCENTAGE ERROR OF THE TWO MODELS AT THE STIFFNESS EXTREMES

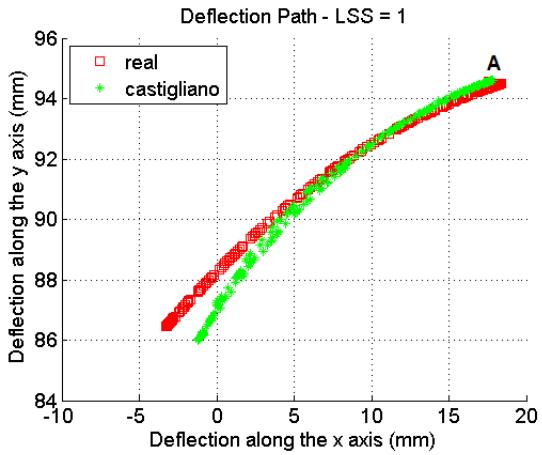

(a)

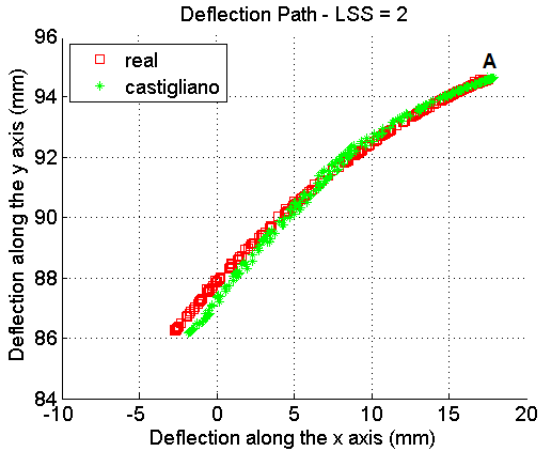

(b)

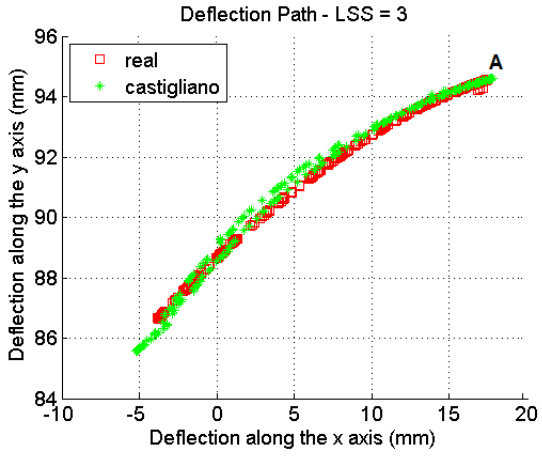

(c)

FIGURE 7. COMPARISION OF THE DEFLECTION PATH OF CASTIGLIANO MODEL WITH REAL DATA AT THE INTERMEDIATE STIFFNESS SETTINGS,(a) LSS1, (b) LSS2 AND (c) LSS3.

TABLE 4. TABLE OF RADIAL STIFFNESS

Radial Stiffness (N/m)			
LSS	Actual	Castigliano	Error%
0	1280	1220	4.7
1	1400	1480	5.7
2	1730	1870	8
3	2300	2100	8.7
4	2600	2300	11.5

Another experiment was performed to measure the deflection range of the leg during dynamic locomotion. In this experiment, a high-speed camera (200 fps) was placed one meter away from the path of Edubot. The robot's motion in the sagittal plane was recorded while it ran at 1.1 m/s. The leg length, which we define as the line length between the hip and the ground, was measured from the video data frame-by-frame during the stance phase. This was repeated for three legs visible to the camera. We interpret these measuments as providing an empirical estimate of the probability distribution over the physical deflections in a typical stride, $PR(length)$. The total expected error of each model is then calculated as

$$\sum_{length} = PE_{model}.Pr(length), \tag{15}$$

where PE_{model} is obtained from Eqn. (14). The results reveal that the total expected error of PRB model is 1.7 times larger than the total expected error of Castigliano's model.

Fig. 8 shows the radial force-deflection relationship of actual data and Castigliano's model at various leg stiffness settings where radial deflection is defined as the deflected radial distance due to the component of the load passing through the center of circle. The maximum radial stiffness, $\frac{F_{y,max}}{\delta_{y,max}}$, of each stiffness setting is given in Tab. 4. The results show that the radial stiffness of the empirical data and Castigliano's model are almost the same at LSS = 0 and 1. At LSS = 2 to 4 there is approximately 10% difference between actual and estimated stiffnesses.

5 CONCLUSION

In this study, the spatial compliance of a tunable C-shaped leg was modeled using Castiglianos Theorem. The results suggest that this approach may represent a simple,

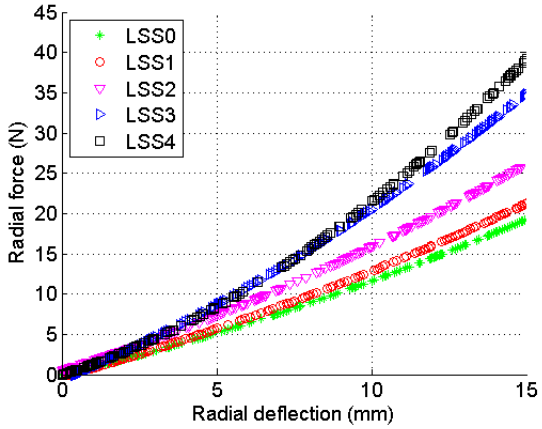

(a)

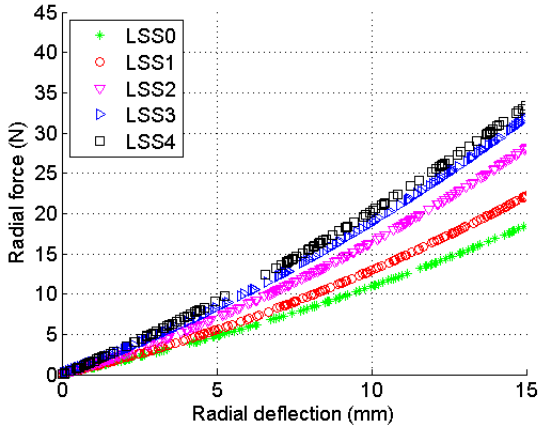

(b)

FIGURE 8. COMPARISION OF THE RADIAL FORCE-DEFLECTION PATH OF ACTUAL AND CASTIGLIANO MODEL FOR ALL STIFFNESS SETTINGS.(a)ACTUAL (b)CASTIGLIANO

accurate, and computationally efficient method for analyzing deflections especially at intermediate leg stiffess settings. This elastic half circular model is a new addition to the existing literature on modeling elastic behavior of the composite C-shaped legs used in the RHex-like class of robots. Until now, all the simulations in the literature we are aware of [1, 15] have modeled the C-legs as linear translational springs, which clearly do not capture the two degree-of-freedom and leg angle dependent stiffness behavior of the C-leg in the sagittal plane. This study convinces us that the Castigliano model may likely yield further insight into the dynamics of physical RHex-like machines equipped with these very effective and apparently simple but, heretofore, poorly modeled legs.

ACKNOWLEDGMENT

Yasemin Özkan Aydın is supported by the International Research Fellowship Program of The Scientific and Technological Research Council of Turkey (TÜBİTAK). This work is also partially supported by the NSF FIBR #0425878.

REFERENCES

[1] Saranli, U., Buehler, M., and Koditschek, D., 2000. "Design, modeling and preliminary control of a compliant hexapod robot". *IEEE International Conference of Robotics and Automation*.

[2] Saranli, U., Buehler, M., and Koditschek, D., 2001. "Rhex: A simple and highly mobile hexapod robot". *International Journal of Robotics Research*, ***20***(7), pp. 616–631.

[3] Moore, E., Campbell, D., Grimminger, F., and Buehler, M., 2002. "Reliable Stair Climbing in the Simple Hexapod RHex". *IEEE International Conference on Robotics and Automation*.

[4] Weingarten, J., Lopes, G., Buehler, M., Groff, R., and Koditschek, D., 2004. "Automated gait adaptation for legged robots". In IEEE International Conference of Robotics and Automation.

[5] Rao, S., 2004. *The Finite Element Method in Engineering*. Elsevier, Burlington,MA.

[6] Howell, L., 2001. *Compliant Mechanisms*. Wiley, New York,NY.

[7] Howell, L., and Midha, A., 1996. "Parametric deflection approximations for initially curved, large-deflection beams in compliant mechanisms". *In Proceedings of the ASME Design Engineering Technical Conference*.

[8] K.C.Galloway, J.E.Clark, and Koditschek, D., 2007. "Design of a multi-directional variable stiffness leg for dynamic running". *In Proceedings of the ASME Design Engineering*.

[9] K.C.Galloway, J.E.Clark, and Koditschek, D., 2009. "Design of a tunable stiffness composite leg for dynamic locomotion". *In Proceedings of the ASME Int.Design Engineering Tech. Conferences*.

[10] Langhaar, H., 1962. *Energy Methods in Applied Mechanics*. John Wiley, New York.

[11] Komsuoglu, H., Sohn, K., Full, R. J., , and Koditschek, D., 2008. "A Physical Model for Dynamical Arthropod Running on Level Ground". *Proc. 11th International Symposium on Experimental Robotic*, pp. 303–317.

[12] Budynas, R., and Nisbett, K., 2008. *Shigley's Mechanical Engineering Design*. McGraw-Hill, New York,NY.

[13] Budynas, R., 1998. *Advanced Strength and Applied Stress Analysis*. McGraw-Hill, New York,NY.
[14] McCormac, J., 2008. *Structural Steel Design*. Pearson Prentice Hall, Upper Saddle River,NJ.
[15] Saranli, U., 2000. SimSect Hybrid Dynamical Simulation Environment. Technical report CSE-TR-437-00, University of Michigan, Ann Arbor, MI. See also URL `http://www.eecs.umich.edu/techreports/cse/00/CSE-TR-436-00.pdf`.